

## **Consistent Late Onset of the Western North Pacific Tropical Cyclone Season Following major El Niño Events**

**Haikun ZHAO**

*Key Laboratory of Meteorological Disaster, Ministry of Education,  
Nanjing University of Information Science and Technology, China  
Joint International Research Laboratory of Climate and Environment Change,  
Nanjing University of Information Science and Technology, China  
Collaborative Innovation Center on Forecast and Evaluation of Meteorological Disaster,  
Nanjing University of Information Science and Technology, China  
Pacific Typhoon Research Center, Nanjing University of Information Science and Technology, China  
Earth System Modeling Center, Nanjing University of Information Science and Technology, China*

**Liguang WU**

*Pacific Typhoon Research Center, Nanjing University of Information Science and Technology, China  
Earth System Modeling Center, Nanjing University of Information Science and Technology, China*

**Chao WANG**

*Key Laboratory of Meteorological Disaster, Ministry of Education,  
Nanjing University of Information Science and Technology, China  
Joint International Research Laboratory of Climate and Environment Change,  
Nanjing University of Information Science and Technology, China  
Collaborative Innovation Center on Forecast and Evaluation of Meteorological Disaster,  
Nanjing University of Information Science and Technology, China  
Pacific Typhoon Research Center, Nanjing University of Information Science and Technology, China  
Earth System Modeling Center, Nanjing University of Information Science and Technology, China*

**and**

**Philip J. KLOTZBACH**

*Department of Atmospheric Science, Colorado State University, Colorado, USA*

*(Manuscript received 3 August 2018, in final form 18 February 2019)*

### **Abstract**

Most studies have focused on variations of tropical cyclone (TC) frequency, intensity, and track over the western North Pacific (WNP), but variability of WNP TC season onset date (TCSO) has been less studied. Recent

---

Corresponding author: Haikun Zhao, Pacific Typhoon Research Center, Key Laboratory of Meteorological Disaster of Ministry of Education, Nanjing University of Information Science and Technology, Nanjing, 210044, China  
E-mail:zhk2004y@gmail.com  
J-stage Advance Published Date: 11 March 2019



research has indicated a close association between WNP TCSO and sea surface temperature (SST) over the tropical Indian Ocean and the tropical central-eastern Pacific. This study has found that relationship between TCSO and SST underwent an inter-decadal change in the late 1990s, likely due to a climate shift that occurred around that time. An observed significant correlation between TCSO and SST before the late 1990s has been insignificant since that time. This was confirmed by the fact that El Niño Southern Oscillation (ENSO) at 0.46 positively correlates with TCSO from 1965–1999 (significant at the 95 % level), and the correlation becomes insignificant (0.16) during 1998–2016. Further analysis suggests that the close association between TCSO and SST is robust only for major El Niño events, with consistently extreme late TCSO following major El Niños during the satellite era. Accompanying the decay of major El Niños, tropical equatorial easterly anomalies in the WNP are driven by a Matsuno–Gill-type response to the specific SST anomaly pattern over the tropical Indo-Pacific sector. This in turn induces an anomalous anticyclone, anomalous westerly vertical wind shear, reduced mid-level moisture and suppressed convection over the WNP basin—all of which are unfavorable for WNP TCs, resulting in delayed TCSO following major El Niño events. These inter-decadal changes in the inter-annual correlation between TCSO and ENSO are largely due to the changing influence of moderate El Niño events on TCSO before and after the late 1990s. This study improves understanding of the ENSO–TC relationship, which should aid seasonal outlooks of WNP TC activity.

**Keywords** extremely late onset; tropical cyclone season; tropical Indian Ocean warming; major El Niño; western North Pacific

**Citation** Zhao, H., L. Wu, C. Wang, and P. J. Klotzbach, 2019: Consistent late onset of the western North Pacific tropical cyclone season following major El Niño events. *J. Meteor. Soc. Japan*, **97**, 673–688, doi:10.2151/jmsj.2019-039.

## 1. Introduction

The western North Pacific (WNP) Ocean including the South China Sea (SCS) is the most active tropical cyclone (TC) basin around the globe on an annually-averaged basis, experiencing about 27 named TCs per year (Chan 2005). Unlike the North Atlantic and eastern North Pacific, the WNP TC season extends across the entire calendar year (Chan 2005). These TCs can cause enormous socio-economic damage and loss of life in China, Japan, Korea and other nations affected by WNP TCs (Zhang et al. 2009). An accurate prediction of the onset date of an active WNP TC season (TCSO) is important for planning that can prevent loss of life and property from TC-associated hazards. However, most prior studies have focused on variations of TC frequency, intensity, and track over the WNP (Lander 1994; Wang and Chan 2002; Camargo and Sobel 2005; Zhao et al. 2010, 2011; Wu et al. 2015), while variability of the WNP TCSO has been relatively less studied.

El Niño Southern Oscillation (ENSO) has been recognized as an important factor of inter-annual variations of WNP TC activity, with a consensus that ENSO has no noticeable impact on total TC frequency but has a significant impact on TC formation location and subsequent track and intensity (Lander 1994;

Wang and Chan 2002; Camargo and Sobel 2005; Zhao et al. 2010, 2011; Wang and Wu 2016; Chen and Wang 2018). A significant southeastward displacement in TC formation is typically observed during El Niño years. These TCs then tend to take a northwestward track, and since they form farther southeast in the basin, they tend to have a longer duration and a stronger lifetime maximum intensity. These changes are largely attributed to a reduced Pacific Walker Circulation during El Niño years that causes favorable large-scale conditions for southeastern WNP TC formations, such as a significant southeastward shift of the WNP monsoon trough (Wang and Chan 2002) and a pronounced eastward retreat of the WNP tropical upper tropospheric trough (TUTT) (Wang and Wu 2016). Accompanied by changes in the TUTT and the monsoon trough over the WNP basin, reduced westerly vertical wind shear and enhanced low-level relative vorticity occur in the eastern part of the WNP basin, which favors more TCs over the eastern portion of the WNP basin. Since there is a significant impact of ENSO on these large-scale conditions over the WNP basin, there is speculation on whether ENSO has a substantial association with inter-annual variations of the WNP TCSO. Recently, following the major El Niño event of 2015–2016 (L’Heureux et al. 2017), an extremely late TCSO over the WNP was observed with the first named TC of

2016 not forming until July 3. One question naturally arises: Are extremely late TCSOs over the WNP closely associated with major El Niño events?

Apart from the impact of ENSO, it has been well documented that tropical Indian Ocean (TIO) sea surface temperatures (SSTs) have a significant influence on the inter-annual variability of WNP TC activity (Du et al. 2009, 2011; Xie et al. 2009, 2016; Zhan et al. 2011; Tao et al. 2012). Xie et al. (2009) suggested that the persistence of basin-wide TIO warming after El Niño decay can stimulate a downwelling (warming) atmospheric Kelvin wave passing across the western Pacific and causing off-equator divergence over the subtropical WNP basin. Du et al. (2011) noted a significant decrease in WNP TC numbers in the summers following major El Niño events (i.e., 1972/1973, 1982/1983, and 1997/1998) and further pointed out that this was predominantly due to TIO warming induced by major El Niño events and its associated impacts on the large-scale environment.

More recently, Takaya et al. (2017) suggested from both observations and numerical simulations that the quiescent TC season in the WNP basin during the early summer (May–July) of 2016 was largely attributed to the warm TIO sea surface temperature anomalies (SSTAs) induced by the preceding 2015/2016 major El Niño event. Kim et al. (2017) analyzed inter-annual variations of the TCSO over the WNP during 1951–2015 and pointed out that it was closely associated with variations of SSTs in the TIO and the central-eastern Pacific (CEP). However, our analysis suggests that the relationship between TCSO over the WNP basin and global SST patterns shows inter-decadal changes, which will be discussed later in this study. This finding cannot be inferred from the analysis of the full period from 1951 to 2015 as was done by Kim et al. (2017). Our analysis further indicated that the robust relationship suggested by Kim et al. (2017) holds true only for major El Niño events. Together with studies on the importance of TIO SSTAs accompanying decay of strong El Niño events, we hypothesize that the persistence of positive TIO SSTAs induced by major El Niño events results in a late TCSO by causing unfavorable large-scale conditions for tropical cyclogenesis in the WNP. In this study, we explore the associated plausible physical causes of the relationship between El Niño events and the extremely late TCSO over the WNP basin.

The remainder of this study is arranged as follows. Section 2 gives descriptions of the data and the methodology used. Section 3 discusses the possible relationship between WNP TCSO and ENSO. Section

4 investigates the physical causes for the extremely late TCSO following major El Niño events, primarily focusing on the substantial impact of changes in the large-scale conditions induced by changes in specific SSTA patterns over the tropical Indo-Pacific sector. Section 5 provides a summary and a discussion.

## 2. Data and methodology

### 2.1 TC data, atmospheric data and SST data

The TC data record was obtained from best track dataset of the United States Joint Typhoon Warning Center (JTWC) (Chu et al. 2002). This dataset provides information on TC location including latitude and longitude and maximum sustained wind speed at six-hour intervals. Our use of data from JTWC is largely based on its more reliable TC intensity estimates than those available from other best track datasets (Wu and Zhao 2012). Due to the availability of satellite observations since 1965, the TC data record since 1965 is considered to be more homogeneous and generally of higher quality. The JTWC dataset also benefited from the availability of reconnaissance aircraft until 1987. While this study mainly covers the satellite era, 1965–2016, we also include some analysis for the period 1951–2016, to compare our results with the full time period investigated by Kim et al. (2017). Only TCs with a maximum sustained wind speed equal to or greater than  $17 \text{ m s}^{-1}$  were considered. Following Kim et al. (2017), we defined a “TC year” in the WNP as the period from February 1 in the corresponding year to January 31 in the following year, which is mainly due to the annual minimum mean monthly TC number in the WNP occurring during February (Kim et al. 2014). The TC season length over the WNP basin [ $0\text{--}30^\circ\text{N}$ ,  $100\text{--}180^\circ\text{E}$ ] including the SCS was identified as the period from the 5th percentile (referred to as the TCSO) to the 95th percentile (referred to as the TC season end) of TC formation dates in each TC year. Annual TC formation dates and their corresponding 5th and 95th percentiles for the TC year from 1951–2016 are displayed with a box-whisker plot (Fig. 1).

Monthly atmospheric variables including winds, relative humidity, relative vorticity, and geopotential height are retrieved from the National Centers for Environmental Prediction (NCEP) Reanalysis I dataset on a  $2.5^\circ \times 2.5^\circ$  latitude-longitude grid (Kalnay et al. 1996). Monthly mean SST is derived from the National Oceanic and Atmospheric Administration Extended Reconstructed SST version 4 (ERSST v4) at a horizontal resolution of  $2^\circ \times 2^\circ$  (Huang et al. 2015, 2016).

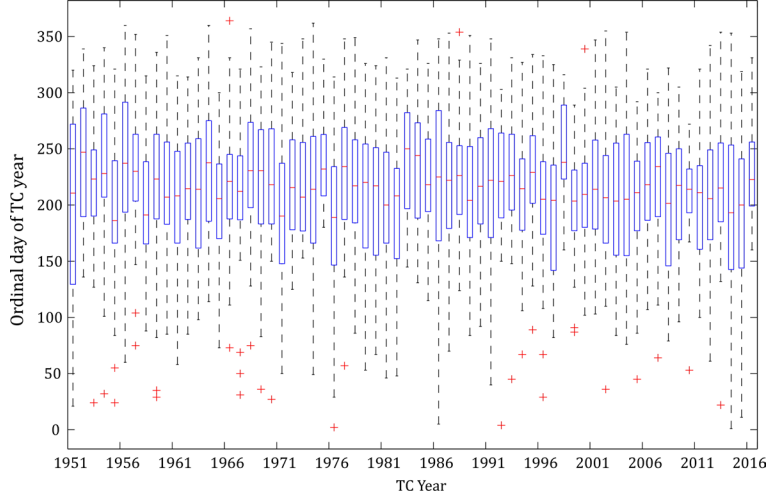


Fig. 1. Box-and-whisker plot for WNP TC formation dates for 1951–2016. The boxes cover from the 25th to the 75th percentiles (lower to upper quartiles, respectively) and the whiskers extend to the 5th and 95th percentiles for the annual TC formation dates.

## 2.2 Genesis potential index

To further assess TCSO over the WNP basin, the genesis potential index (GPI) was used as a diagnostic tool to assess the relative importance of the large-scale controls of TC activity. In this study, we adopted the GPI developed by Emanuel and Nolan (2004) with the following expression:

$$\text{GPI} = |10^5 \xi|^{3/2} \times \left( \frac{H}{50} \right)^3 \times \left( \frac{V_{pot}}{70} \right)^3 \times (1 + 0.1 \times V_{shear})^{-2}, \quad (1)$$

where  $\xi$  is the 850 hPa absolute vorticity ( $s^{-1}$ ),  $H$  is the 600 hPa relative humidity (%),  $V_{pot}$  is the potential intensity (PI) ( $m s^{-1}$ ), providing a theoretical upper bound on TC intensity (Bister and Emanuel 2002), and  $V_{shear}$  is the vertical wind shear, computed as the magnitude of the vector difference between 850 hPa and 200 hPa ( $m s^{-1}$ ). The respective role of each of the four factors included in the GPI in contributing to the extremely late TCSO is assessed according to Camargo et al. (2007). The GPI is calculated by varying one variable but keeping the other three variables at their climatological values for the period 1965–2016. They are referred to as GPI-RH, GPI-VOR, GPI-SHEAR, and GPI-PI, respectively, indicating the distinct contributions from the mid-level relative humidity, low-level absolute vorticity, vertical wind shear and PI. The GPI with all four varying variables is referred to as the GPI-Total. Although the net anomaly cannot be

described as the sum of the individual contributions of the four factors included in the GPI because of its nonlinearity, the index can provide an adequate quantification of the role of each of the different factors. This methodology has been adopted in several previous studies (Camargo et al. 2009; Jiang et al. 2012; Zhao et al. 2014, 2015a, b, 2017).

## 2.3 Statistical significance

A compositing technique is used to explore the plausible causes associated with the extremely late TCSO following major El Niño events. The non-parametric Mann–Kendall test (Mann 1945; Kendall 1975) and the Wilcoxon–Mann–Whitney test (Wilcoxon 1945; Mann and Whitney 1947) were used to assess the statistical significance of the correlation and the difference, respectively.

To evaluate the significance of the percentages on an early or late onset of the TC season for different ENSO intensities, the bootstrap test was adopted. In bootstrap tests, null cases were identified using the dates of all TC genesis events except the samples in the tested category. Null composites were generated by randomly selecting the same number of dates from the null cases as had been in the tested category. This procedure was repeated to calculate 1000 null composites. In this study, we stratify the December–February average (DJF) Niño-3.4 index into four categories: strong El Niño ( $\text{Niño-3.4} \geq 1.5\sigma$ ;  $\sigma$  is the standard deviation), moderate El Niño ( $0.6\sigma \leq \text{Niño-3.4} < 1.5\sigma$ ), weak El Niño ( $-0.5\sigma \leq \text{Niño-3.4} < 0.6\sigma$ ), and La Niña ( $\text{Niño-3.4} < -0.5\sigma$ ).

Table 1. Statistics for the onset date, end date, and length of the TC season over the WNP basin for two periods: **P1:1951–2016** and **P2:1965–2016**. The ordinal date is the count of days from 1 February (0) to 31 January (+1). Asterisks (\*\*) denote that the correlation coefficient is significant at the 95 % confidence level. The sign “++” indicates a significant trend at the 95 % confidence level. The TC season onset date and end are the 5th and 95th percentiles of TC formation dates in the TC year, and the season length is the period between the season onset date and the season end date.

	Average (P1/P2)		Standard deviation (days) (P1/P2)	Correlation coefficient during P1/P2			Trend (days yr <sup>-1</sup> ) (P1/P2)
	Ordinal date	Calendar date		Season end	Season length	Annual TC counts	
Season onset	108/110	18 May/20 May	34.5/33.9	0.23/0.33	<b>−0.85**/−0.84**</b>	0.01/−0.15	0.23/−0.04
Season end	300/299	28 Nov./27 Nov.	19.1/19.1		0.27/0.24	−0.07/−0.01	−0.25/−0.15
Season length	193 days/ 189 days		35.2/32.9			0.05/0.15	<b>−0.48++/−0.11</b>

$3.4 < 1.5\sigma$ ), neutral ENSO ( $−0.6\sigma < \text{Ni}\tilde{\text{o}}\text{-}3.4 < 0.6\sigma$ ) and La Niña ( $\text{Ni}\tilde{\text{o}}\text{-}3.4 \leq −0.6\sigma$ ).

### 3. TCSO–ENSO association

Table 1 presents statistics derived for the satellite era (1965–2016) and for the full period investigated in Kim et al. (2017): 1951–2016. The average TCSO date is May 18, and the average TC season end date is November 28 based on the full period (1951–2016). Annual TC counts from 1951 to 2016 have a weak correlation with TCSO, TC season end and TC season length. There are no significant trends in TCSO, TC season end and TC season length since 1951. As would be expected, TC season length is significantly correlated with TCSO. These results are consistent with results presented by Kim et al. (2017), with some slight differences due to the different TC dataset (from the Japan Meteorological Agency) used by Kim et al. (2017).

Several studies have highlighted the uncertainties in TC data over the WNP basin during the pre-satellite era (Landsea 2007; Landsea et al. 2010; Song et al. 2010; Wu and Zhao 2012), so it is worth comparing results derived for two different periods: 1951–2016 and 1965–2016. As can be seen in Table 1, significant differences are clearly observed when comparing the results for the whole period from 1951–2016 and for only the satellite era from 1965 to 2016. For example, the positive trend of TCSO over the WNP during 1951–2016 is larger in magnitude than that during 1965–2016. A significant decreasing trend of TC season length can be found during 1951–2016, but this trend becomes insignificant when one only looks at TC season length from 1965–2016. Significant correlations between TCSO and TC season length can be found for both periods (−0.85 for 1951–2016 and −0.84 for 1965–2016), whereas TC season end is only

weakly correlated with TC season length (0.27 for 1951–2016 and 0.24 for 1965–2016). Consequently, TC season length variability largely depends on TCSO and is less dependent on TC season end. Annual TC counts have a weak correlation with TCSO, TC season end and TC season length.

Further examination suggests that the differences highlighted in Table 1 are largely due to the uncertainty of TCSO during the pre-satellite era. Indeed, a significantly earlier TCSO (i.e., 7 May) can be found during the pre-satellite era (i.e., 1951–1964) compared to the TCSO (i.e., 22 May) during the post-satellite era (i.e., 1965–2016). This result is further confirmed by distinct correlation patterns between the TCSO and December–February averaged (DJF) SSTs between 1951–2016 and 1965–2016 (Fig. 2). A clear difference over the TIO can also be readily seen with significant correlations from 1951 to 2016 but insignificant correlations over the more recent period from 1965 to 2016. Significant correlations over the CEP are found during both periods. The results of this comparison over different periods led us to choosing the satellite era period from 1965 to 2016 for the analyses in this study. The differences highlighted in Table 1 and Fig. 2 between the periods provide further evidence that our results and those reported by Kim et al. (2017) are different.

Figure 3a shows time series of TCSO over the WNP basin and ENSO, represented by the averaged DJF Niño-3.4 index. The correlation between TCSO and ENSO is 0.37, is significant at the 95 % confidence level and is consistent with that by Kim et al. (2017). An inter-decadal change of the inter-annual relationship between ENSO and TCSO is found around the late 1990s, identified by a change-point analysis of 13-year sliding correlations between the two time series (Fig. 4). This climate regime shift has been reported

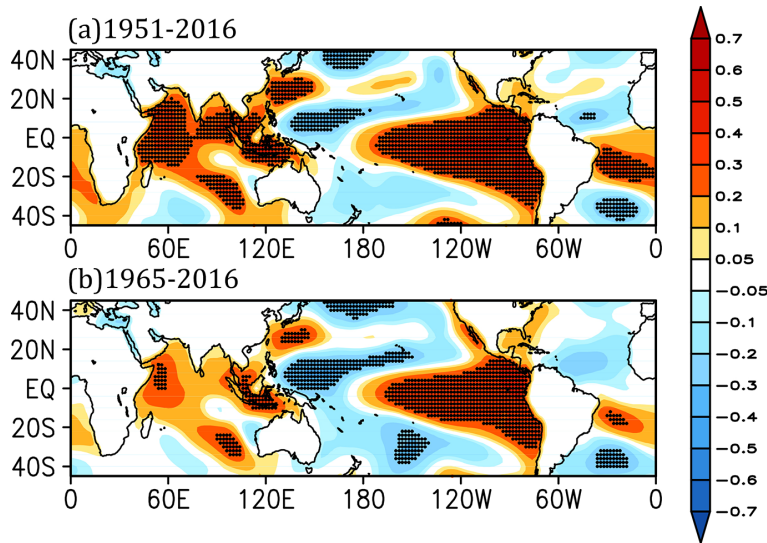


Fig. 2. Correlation pattern between TC season onset date over the WNP basin and December-February-averaged (DJF) SSTs for 1951–2016 and 1965–2016, respectively. The “stippling” indicates that the value is significant at the 95 % confidence level.

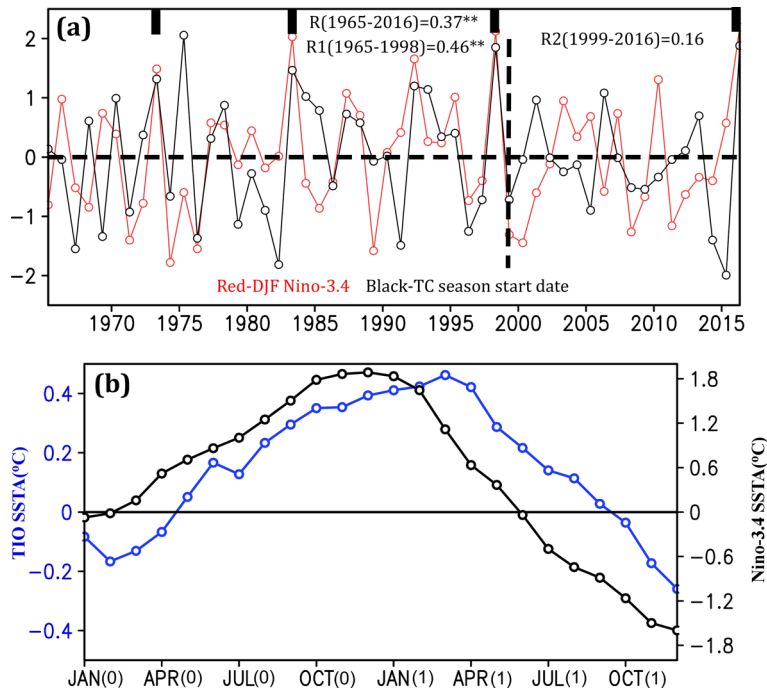


Fig. 3. (a) Inter-annual correlation between the standardized onset date of the WNP TC season and the December-February (DJF) Niño-3.4 index. Correlations during 1965–2016, 1965–1998 and 1999–2016, respectively, are 0.37 (significant at the 95 % confidence level), 0.46 (significant at the 95 % confidence level) and 0.16 (not significant at the 95 % confidence level). (b) Evolution of SST anomalies over the Niño-3.4 region and tropical Indian Ocean compositing on four strong El Niño events (i.e., 1972/1973, 1982/1983, 1997/1998, and 2015/2016).

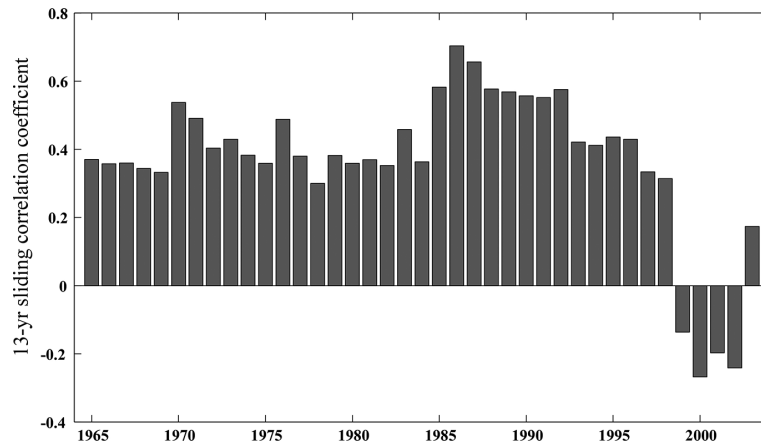


Fig. 4. 13-yr sliding correlations between TC season onset date (TCSO) over the WNP basin and the December–February (DJF) Niño-3.4 index during the period of 1965–2016.

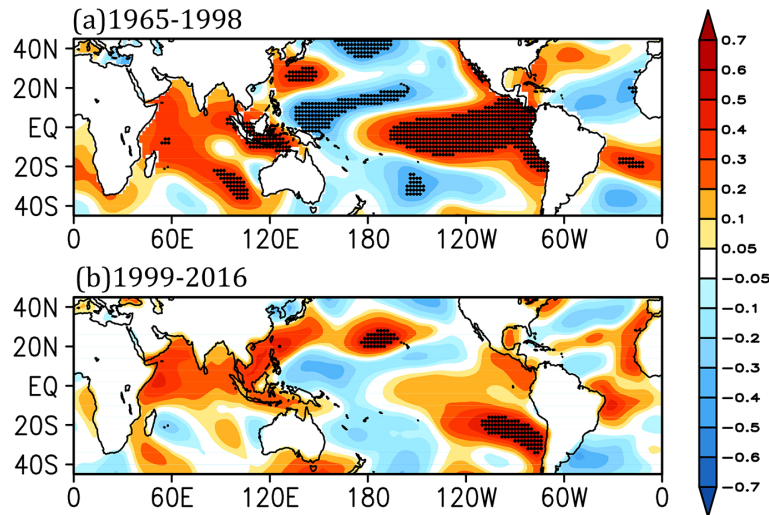


Fig. 5. Correlation pattern between TC season onset date over the WNP basin and December–February-averaged (DJF) SSTs for 1965–1998 (a) and 1999–2016 (b). The “stippling” indicates that the value is significant at the 95 % confidence level.

in many previous studies (Tu et al. 2009; Maue 2011; Kosaka and Xie 2013; Liu and Chan 2013; Xiang et al. 2013; Hong et al. 2014, 2016; England et al. 2014; Zhao and Wang 2016). For example, there is evidence that links the regime shift of ENSO during the recent decades to the decadal variations in the mean state of the Pacific associated with the PDO transitions from a warm to a cool phase since the late 1990s (Verdon and Franks 2006; Kao and Yu 2009; Cai et al. 2014; Xiang et al. 2013; Liu and Chen 2018). The large-scale environmental changes associated with this

regime shift have been well documented (Xiang et al. 2013; Hong et al. 2014, 2016; Zhao and Wang 2016, 2018; Hu et al. 2016, 2018). Note that ENSO at 0.46 positively correlates with TCSO from 1965–1999 (significant at the 95 % level), whereas the correlation becomes insignificant (0.16) since 1999. Such an inter-decadal shift in the TCSO–ENSO relationship is clearly displayed when examining the correlation maps during both time periods (Fig. 5). Correlations are generally much weaker from 1999–2016 than they were from 1965–1998.

Table 2. Statistics for the counts of early or late onset of the TC season over the WNP basin for the two periods before and since the climate regime shift: 1965–1998 and 1999–2016, as a function of different ENSO magnitudes and their respective percentages. Here the early or late TC season onset depends on the anomalies of the TC season onset date before and since 1998. The significance of their percentages for different ENSO flavors is evaluated using a 95 % bootstrap confidence level.

ENSO flavors	1965–1998		1999–2016		Significance (95 %)	
	Late onset	Early onset	Late onset	Early onset	Late onset	Early onset
Strong El Niño [Niño 3.4 ≥ 1.5σ]	3/3 (100 %)	0/3 (0 %)	1/1 (100 %)	0/1 (0 %)	×	×
Moderate El Niño [0.6σ < Niño-3.4 < 1.5σ]	4/6 (67 %)	2/6 (33 %)	1/4 (25 %)	3/4 (75 %)	✓	✓
Neutral ENSO [-0.6σ < Niño-3.4 < 0.6σ]	7/16 (44 %)	9/16 (56 %)	3/6 (50 %)	3/6 (50 %)	×	×
La Niña [Niño3.4 ≤ -0.6σ]	5/9 (56 %)	4/9 (44 %)	4/7 (57 %)	3/7 (43 %)	×	×

Further analysis suggests that an inter-decadal change of the inter-annual ENSO–TCSO relationship is largely due to the differing influence of moderate El Niño events (1966, 1969, 1987, 1988, 1995, 2003, 2005, 2007, and 2010) on the TCSO before 1999 and since 1999. When all of the moderate El Niño years are excluded, the inter-annual correlation between ENSO and TCSO shows no significant inter-decadal change, with insignificant correlation coefficients of 0.18 and −0.24 during 1965–1998 and 1999–2016, respectively. Additionally, TCSO following moderate El Niño events occurs after the average TCSO date 67 % of the time from 1965 to 1998, but only 33 % of the time during 1999–2016 (Table 2). This difference of TCSO is significant at the 95 % confidence level. By contrast, no significant differences can be found for neutral and La Niña years (Table 2). Moreover, such an inter-decadal change of the impacts of moderate El Niño events on TCSO is closely associated with significant inter-decadal changes of the large-scale circulation in response to shifts in the climate mean state (Fig. 6). Before 1999, an intensified easterly anomaly is observed throughout the tropical western WNP extending into the TIO, and enhanced westerly anomalies over the eastern WNP are observed for April–June (Fig. 6a), whereas no such anomalies are found since 1999 (Fig. 6b). The changes in the large-scale circulation can be more clearly seen when the differences between the two sub-periods are examined (Fig. 6c). Similar inter-decadal changes are observed for January–March before and since 1999, although their differences are smaller than those during April–June (Figs. 6d–f). These are consistent with TCSO tending to be late (early) before (since) 1999 following mod-

erate El Niño events. Based upon these analyses, we speculate that the current climate regime shift exerts a distinct inter-decadal modulation of the ENSO–TCSO relationship. It is beyond the scope of this study to explore the associated underlying physical mechanism.

The robust ENSO–TCSO relationship holds true for major El Niño events throughout the satellite era. As shown in Fig. 3a, following the four major El Niño events since 1965 (i.e., 1972/1973, 1982/1983, 1997/1998, and 2015/2016), consistently extreme late TCSO (i.e., later than 90 % of TCSO) occurs. In the following section, we focus on investigating how major El Niño events are linked with the extremely late TCSO over the WNP basin. Composite analyses are conducted based on the four major El Niño events in the satellite era (1972/1973, 1982/1983, 1997/1998, and 2015/2016). We denote the ENSO-developing year as year (0) and the following year as year (1). Since the extremely late TCSO following all four major El Niño events occurs during late June or early July, we focus on the comparisons for the following winter-early spring from January to March (JFM(1)) and spring-early summer from April to June (AMJ(1)).

#### 4. Physical causes of extremely late TCSO associated with major El Niño events

##### 4.1 Changes in SST patterns

Figure 3b shows the composite evolution of Niño-3.4 and TIO SSTAs from year (0) to year (1). The TIO anomalously warms following the peak of major El Niño events, as also shown in previous studies (Du et al. 2009; Xie et al. 2009). Niño-3.4 SSTAs anomalously warm during boreal summer (0), peak in December (0) and then subsequently anomalously

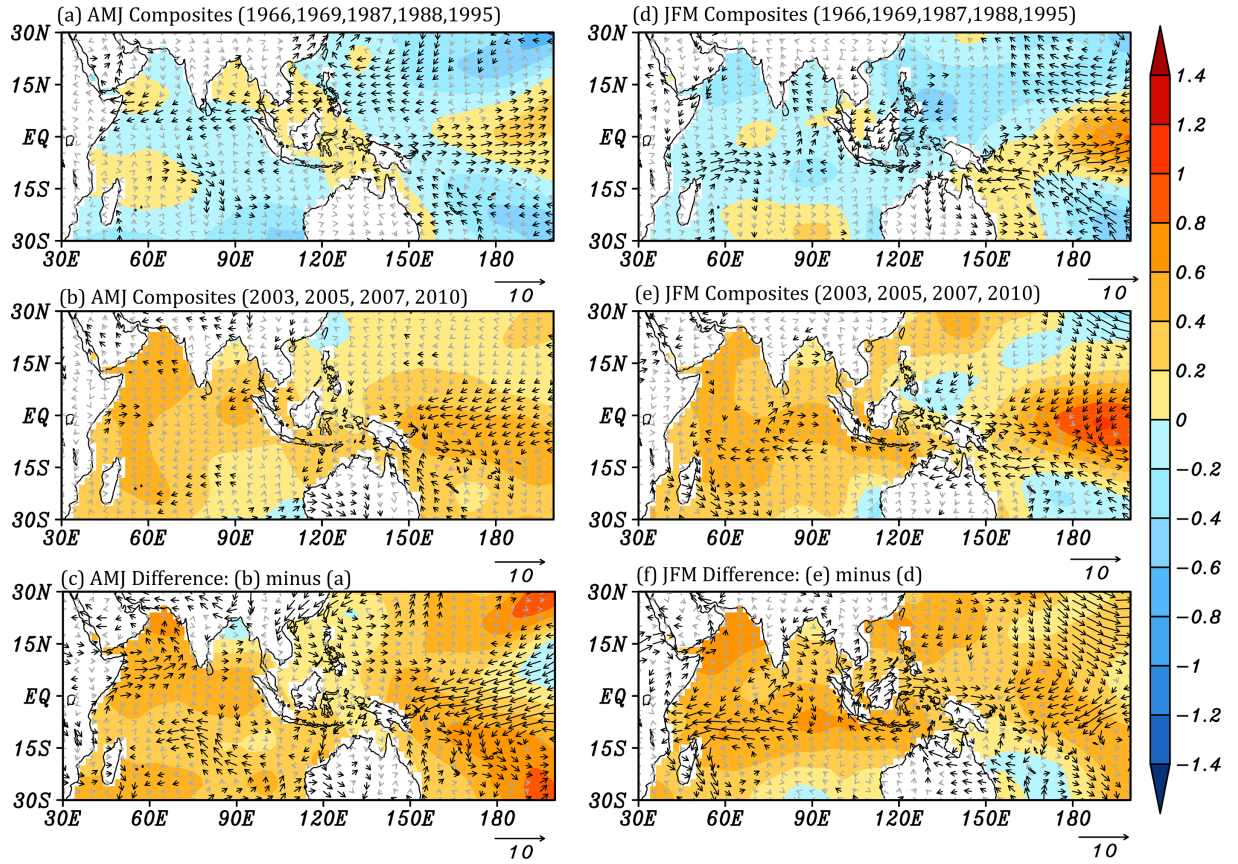


Fig. 6. Composite 850-hPa winds (vectors; unit:  $\text{m s}^{-1}$ ) and sea surface temperature anomalies (SSTA) (shading; unit:  $^{\circ}\text{C}$ ) over April–June in moderate El Niño events prior to the climate shift (i.e., 1966, 1969, 1987, 1988, and 1995) (a) moderate El Niño events since the climate shift (2003, 2005, 2007, and 2010) and their differences (i.e., b minus a). (d and e) are the same as (a and b) except for from January–March, and (f) their differences (i.e., e minus d). The vectors in black are significant at the 95 % confidence level.

cool; by contrast, the TIO anomalous peaks warm in March (1), or have about a one-season lag from Niño 3.4. During JFM (1), moderate positive SSTAs over the CEP and basin-wide positive SSTAs over the TIO are observed. By AMJ (1), although the TIO SSTA decreases, the TIO SSTA remains above normal. Meanwhile, central-eastern Pacific SSTAs anomalously cool to just slightly above normal by AMJ (1).

The persistent TIO warming accompanying the decay of major El Niño events is expected to have significant impacts on large-scale oceanic/atmospheric circulation patterns. Indeed, a sharp contrast in the SST gradient (SSTG) between the warming SSTAs over TIO and cooling SSTAs over the WNP can be readily observed over AMJ (1) when a major El Niño is decaying, with weak positive SSTAs over the far eastern Pacific (Figs. 7a, b). Such a sharp contrast of

SSTA is even clearer in JFM (1) (Figs. 7c, d). The localized TIO warming forms a spatial pattern reminiscent of the Matsuno–Gill-type response pattern, with the warm atmospheric Kelvin wave-induced easterly anomalies expanding westward and penetrating into the western Pacific near the equator. This then induces off-equator low-level divergence over the subtropical WNP from the following spring into the early summer (Fig. 7). This then intensifies the prevailing trades over the WNP basin, causing an anomalous western Pacific anticyclone. Additionally, the observed robust anomalous western Pacific anticyclone from spring to early summer following major El Niño events may be due to local air–sea interaction as suggested by Wang et al. (2000). Major El Niño events consequently then impact the East Asian monsoon circulation.

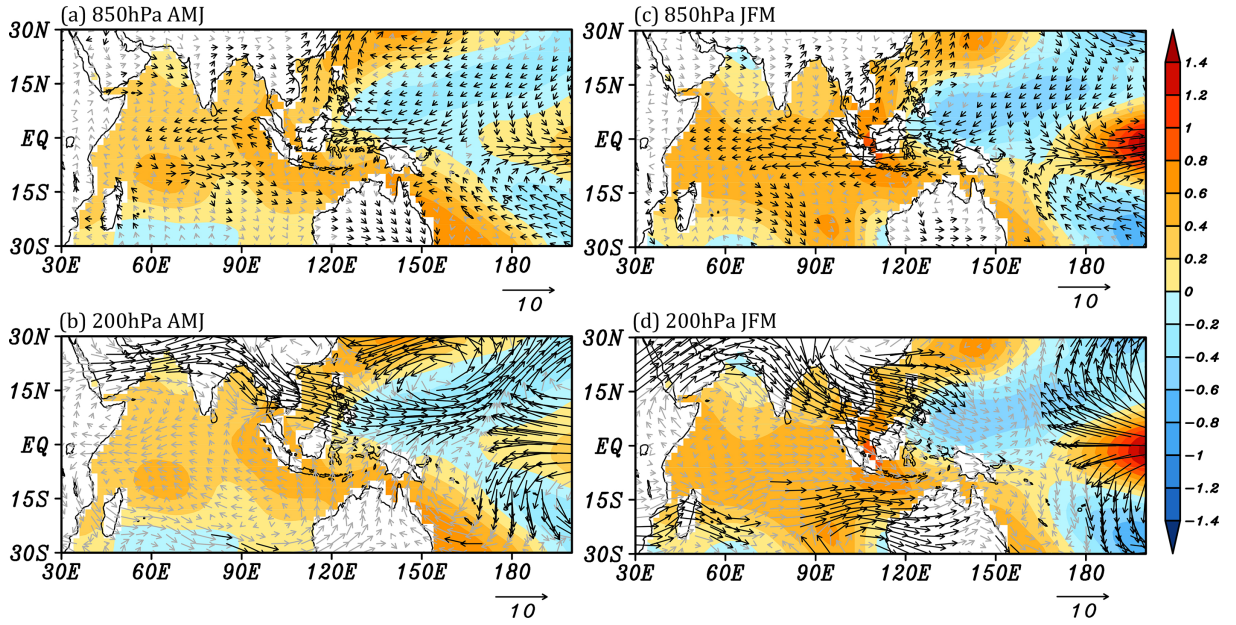


Fig. 7. Composited anomalies over April–June in four strong El Niño events (i.e., 1972/1973, 1982/1983, 1997/1998, and 2015/2016) for (a) 850-hPa winds (vectors; unit:  $\text{m s}^{-1}$ ) and sea surface temperature anomalies (SSTA) (shading; unit:  $^{\circ}\text{C}$ ), and (b) 200-hPa winds (vectors; unit:  $\text{m s}^{-1}$ ) and SSTA (shading; unit:  $^{\circ}\text{C}$ ). (c) and (d) are the same as (a) and (b) except for from January–March. The vectors in black are significant at the 95 % confidence level.

#### 4.2 Changes in large-scale conditions

Robust cyclonic circulation anomalies are seen over the WNP from spring to early summer following major El Niño events (Fig. 7), which are driven by the Matsuno–Gill-type response to the specific SSTA pattern over the tropical Indo–Pacific region. Associated with the anomalous Walker Circulation are corresponding changes in large-scale conditions across the WNP from spring to early summer. Over AMJ (1), a significant anomalous westerly vertical wind shear over the WNP basin is observed (Fig. 8a), largely due to changes in upper-level wind anomalies (Fig. 7b). Meanwhile, anomalous subsidence over the WNP basin associated with the anomalous Walker circulations (Fig. 9a) further reduces mid-level moisture (Fig. 10a) and thus suppresses convection over the WNP basin. The WNP subtropical high also has a significant westward extension (Fig. 11a). These changes in large-scale conditions are unfavorable for TC genesis over the WNP basin. All of these large-scale factors are more unfavorable for TC genesis over JFM (1) compared to that over AMJ (1) except for vertical wind shear (Figs. 7d, 8b, 9b, 10b, 11b). Over JFM (1), moderate enhanced vertical wind shear can be found over the main development region

for TCs (Fig. 8b). As suggested by previous studies (Matsuno 1966; Newell et al. 1973; Gill 1980), the anomalous circulation in Figs. 7 and 8 is essentially maintained by the east–west differential heating generated by the SST anomalies (Fig. 7) through the east–west circulation (Fig. 9). In summary, observational analyses suggest that the persistence of basin-wide TIO warming induced by major El Niño events and east–west differential heating generated by the SSTA pattern force low-level anomalous easterlies in the western Pacific and in turn cause unfavorable large-scale conditions from spring to early summer leading to a delayed TCSO. These results are consistent with previous studies on the importance of the TIO for the WNP climate (Du et al. 2009, 2011; Xie et al. 2009; Zhan et al. 2011; Tao et al. 2012).

#### 4.3 Relative importance of environmental factors

As discussed above, major El Niño events can lead to extremely late WNP TCSO through alterations of environmental factors. To explore the relative importance of large-scale factors affecting tropical cyclogenesis from the spring to early summer following major El Niño events, we now conduct a budget analysis of the GPI using an approach similar to that

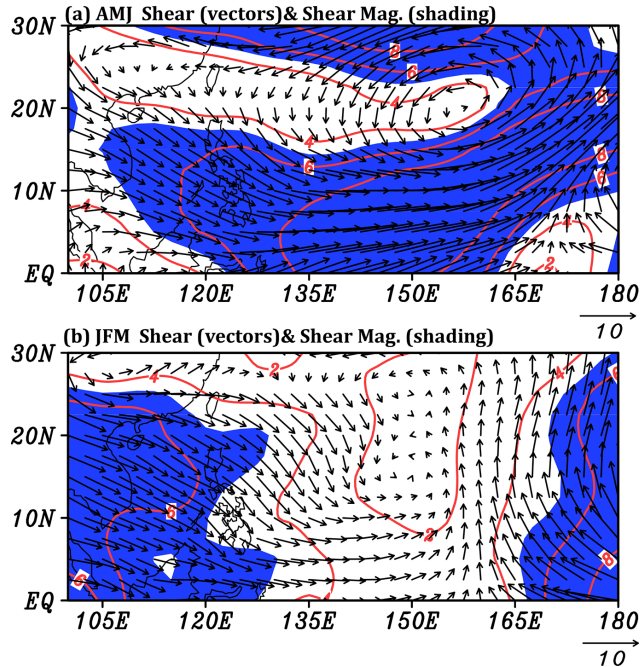


Fig. 8. Composited anomalies over April-June (a) and January-March (b) in four strong El Niño events (i.e., 1972/1973, 1982/1983, 1997/1998, and 2015/2016) for (a) vertical wind shear (200-hPa-850-hPa) and its magnitude (unit:  $\text{m s}^{-1}$ ). The shading indicates that the values are significant at the 95 % confidence level.

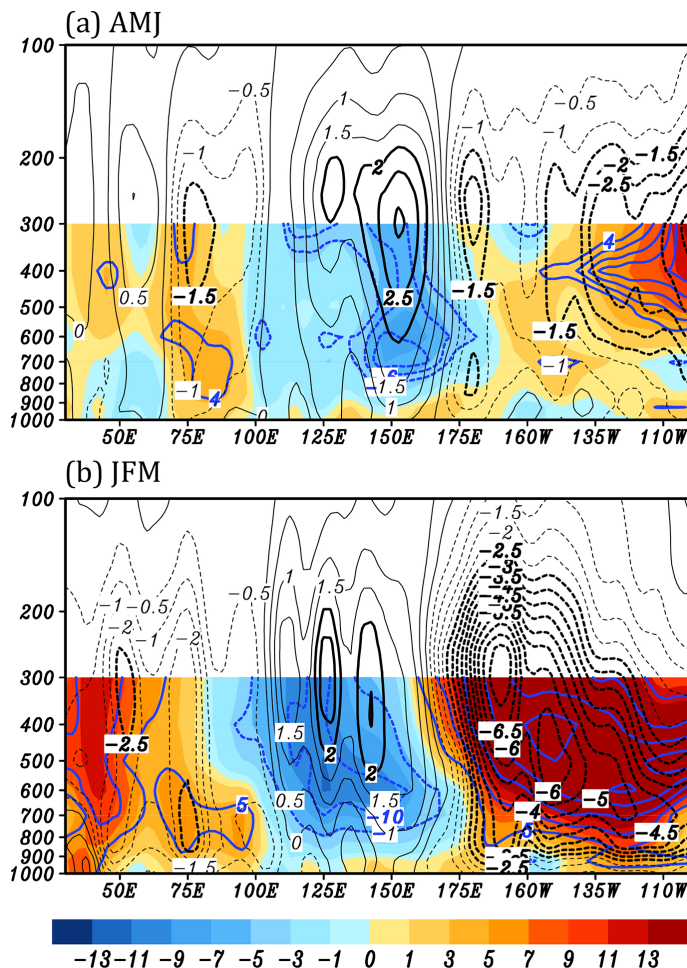


Fig. 9. Composite of relative humidity anomalies (%), shading) and vertical velocity anomalies (contour; unit:  $\text{Pa s}^{-1}$ ) averaged from the equator to  $10^\circ\text{N}$  over April-June (a) and January-March (b) in four strong El Niño events (i.e., 1972/1973, 1982/1983, 1997/1998, and 2015/2016). The contours in blue and in bold-black, respectively, indicate that the relative humidity anomalies and vertical velocity anomalies are significant at the 95 % confidence level.

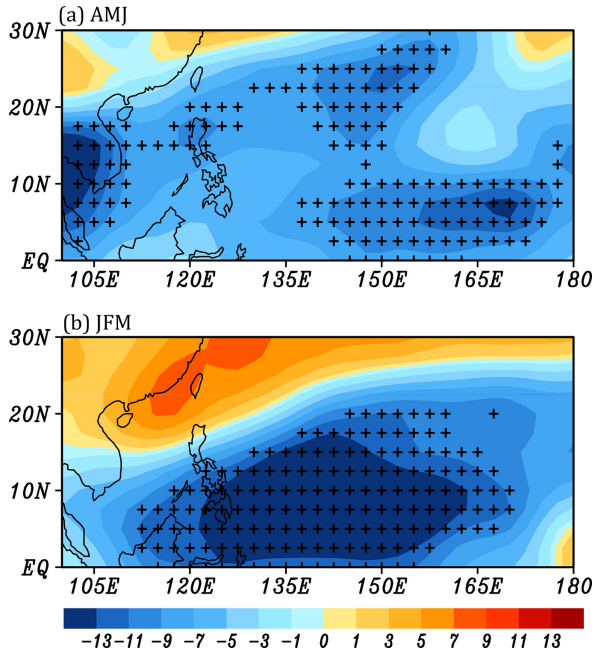


Fig. 10. Composites of 600-hPa relative humidity anomalies (%) (shading) averaged for April–June (a) and January–March (b) in four strong El Niño events (i.e., 1972/1973, 1982/1983, 1997/1998, and 2015/2016). The sign “+” indicates the value is significant at the 95 % confidence level.

of Camargo et al. (2007, 2009).

A significant decrease of GPI can be seen over most of the WNP basin [ $5\text{--}20^{\circ}\text{N}$ ,  $100\text{--}180^{\circ}\text{E}$ ] in both JFM (1) and AMJ (1), which is consistent with the extremely late WNP TCSO following these four major El Niño events (Fig. 12). This result increases our confidence in assessing the relative contribution of large-scale factors to the suppressed TCs for JFM (1) and AMJ (1). Such factors’ relative importance is demonstrated by comparing the magnitudes of the GPI while varying the factors over the WNP basin. As shown in Fig. 12, the decreased GPI-Total over JFM (1) and AMJ (1) is a combined effect of all four of the variables included in the GPI. During AMJ (1), the change of vertical wind shear and mid-level relative humidity appear to be the two most important factors, followed by the low-level vorticity and PI terms (Fig. 12a). During JFM (1), however, the mid-level moisture remains an important factor with secondary contributions from the low-level vorticity and PI terms. Vertical wind shear appears to be relatively less important in JFM (Fig. 12b). Results based upon anal-

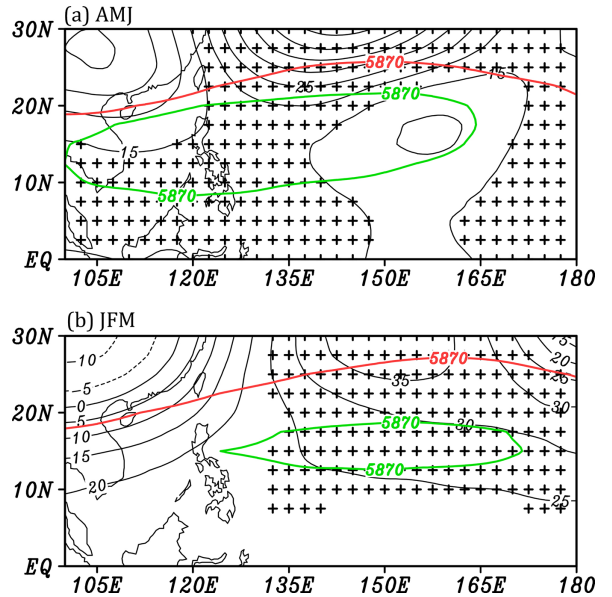


Fig. 11. Composites of 500-hPa geopotential height anomalies (contour; unit: gpm) and the 5870 meter geopotential height line (red) averaged for April–June (a) and January–March (b) in four strong El Niño events (i.e., 1972/1973, 1982/1983, 1997/1998, and 2015/2016). The 5870 meter geopotential height line is in green for the composite of four strong El Niño events and in white for the climatological value from 1970–2016. The sign “+” indicates that the value is significant at the 95 % confidence level.

yses of the GPI agree well with the changes in large-scale factors, further confirming that major El Niño events tend to drive extremely late TCSO over the WNP by causing unfavorable large-scale conditions across the WNP basin.

## 5. Summary and discussion

Current seasonal outlooks of TC activity primarily focus on TC frequency and intensity (Camargo et al. 2007; Klotzbach 2007; Zhan et al. 2011), and significantly less attention has been paid to TCSO, although TCSO has been recently investigated for the North Atlantic basin (Karloski and Evans 2016). TCSO is an important parameter for TC seasonal prediction and risk prevention.

In particular, we focus on the relationship between SSTAs associated with ENSO and TCSO and on the changes that the relationship experienced due to the climate shift that occurred in the late 1990s. Recently,

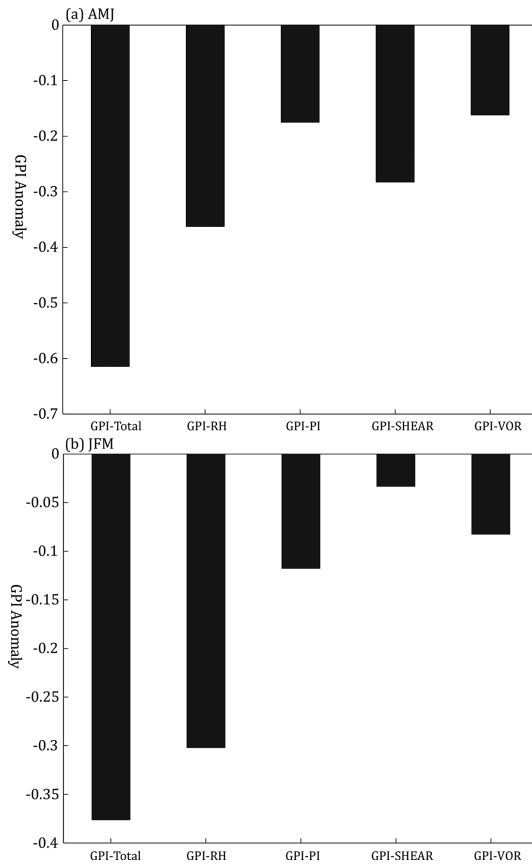


Fig. 12. Composites of GPI-Total and GPI anomalies with the four individually varying factors over the WNP basin averaged for (a) April–June and (b) January–March in four strong El Niño events (i.e., 1972/1973, 1982/1983, 1997/1998, and 2015/2016).

Kim et al. (2017) suggested a close relationship between TCSO and SSTs over both the TIO and CEP when investigating the period from 1951 to 2015. Our results show different results when comparing the periods 1951–2016 and 1965–2016 indicating that the ENSO–TCSO relationship depends on the period selected for analysis (see Table 1, Fig. 2). Given the caveats that other studies have reported on the usage of pre-satellite TC data in the WNP basin, we thought it was best to use the period 1965–2016 to avoid potential erroneous results due to data inhomogeneities prior to continuous satellite monitoring capabilities. Our results suggest that the relationship between ENSO and TCSO during the satellite era experiences an inter-decadal change in the late 1990s, at a time when other studies have also indicated a climate

regime shift. Interestingly, the robust relationship between ENSO and TCSO, also suggested by Kim et al. (2017), holds true only for major El Niño events (i.e., 1972/1973, 1982/1983, 1997/1998, and 2015/2016). Our results suggest that changes in the SSTA pattern over the tropical Indo–Pacific sector associated with major El Niño events play an important role in controlling the extremely late TCSO over the WNP basin.

The persistence of major El Niño-induced TIO warming forces anomalous easterlies across the western Pacific, which then causes off-equator anticyclonic circulation anomalies over the WNP basin. This result is consistent with those of previous studies on the importance of sustained TIO warming on Pacific climate (Xie et al. 2009; Du et al. 2011). The accompanying anomalous upper-level cyclone is clearly observed, which leads to anomalous westerly vertical wind shear over the WNP basin that strengthens the magnitude of vertical wind shear from the preceding winter to the following early summer. Additionally, these SSTAs cause an anomalous Walker-like circulation with anomalous subsidence and reduced mid-level moisture, resulting in suppressed convection across the WNP basin. Owing to the impact of sustained basin-wide TIO warming following the decay of a major El Niño event, these changes in large-scale conditions over the WNP from JFM(1) to AMJ(1) are generally unfavorable for WNP TC activity.

Additionally, our results indicate that the changing influence of moderate El Niño events on TCSO before and since the late 1990s largely contribute to the inter-decadal change of the ENSO–TCSO relationship. In this sense, such an inter-decadal change of the ENSO–TCSO relationship may be associated with changes in the mean climate state. It is worth noting that only observational analyses were conducted in this study, and numerical simulations are needed to test hypotheses about plausible mechanisms leading to the extremely late TCSO following major El Niño events and to confirm the role of changes in the mean climate state. Moreover, another extremely late TCSO over the WNP basin was observed in 1974/1975 (Fig. 3a), which was not a major El Niño event but was rather a La Niña event. This suggests that other factors may be associated with extremely late TCSO. The detailed underlying mechanisms of extremely late TCSO over the WNP basin need further research.

As a final note, this study documents a strong relationship between major El Niño events and extremely late TCSO over the WNP basin. Therefore, we can expect an extremely late TCSO over the WNP basin in the year following a major El Niño event. Studies have

suggested that the occurrence of major El Niño events may show a large increase in the future in response to global warming (Cai et al. 2014). Considering a projected large increase in major El Niño events, we would then expect more frequent extremely late WNP TCSO, which may have important implications for projections of the 21st century TC activity over the WNP.

### Acknowledgments

This research was jointly supported by the National Natural Science Foundation of China (41675072 and 41730961), the Qinglan Project of Jiangsu Province (R2017Q01), the Natural Science Foundation of Jiangsu Province (BK20170941), and the Priority Academic Program Development of Jiangsu Higher Education Institutions (PAPD). P. Klotzbach would like to acknowledge a grant from the G. Unger Vetlesen Foundation.

### References

- Bister, M., and K. A. Emanuel, 2002: Low frequency variability of tropical cyclone potential intensity. 1. Interannual to interdecadal variability. *J. Geophys. Res.*, **107**, 4801, doi:10.1029/2001JD000776.
- Cai, W., S. Borlace, M. Lengaigne, P. van Rensch, M. Collins, G. Vecchi, A. Timmermann, A. Santoso, M. J. McPhaden, L. Wu, M. England, E. Guilyardi, and F.-F. Jin, 2014: Increasing frequency of extreme El Niño events due to greenhouse warming. *Nat. Climate Change*, **4**, 111–116.
- Camargo, S. J., and A. H. Sobel, 2005: Western North Pacific tropical cyclone intensity and ENSO. *J. Climate*, **18**, 2996–3006.
- Camargo, S. J., K. A. Emanuel, and A. H. Sobel, 2007: Use of a genesis potential index to diagnose ENSO effects on tropical cyclone genesis. *J. Climate*, **20**, 4819–4834.
- Camargo, S. J., M. C. Wheeler, and A. H. Sobel, 2009: Diagnosis of the MJO modulation of tropical cyclogenesis using an empirical index. *J. Atmos. Sci.*, **66**, 3061–3074.
- Chan, J. C. L., 2005: Interannual and interdecadal variations of tropical cyclone activity over the western North Pacific. *Meteorol. Atmos. Phys.*, **89**, 143–152.
- Chen, G., and K. Wang, 2018: Why is the tropical cyclone activity over the western North Pacific so distinct in 2016 and 1998 following super El Niño events? *J. Meteor. Soc. Japan*, **96**, 97–110.
- Chu, J.-H., C. R. Sampson, A. S. Levine, and E. Fukada, 2002: *The joint typhoon warning center tropical cyclone best-tracks, 1945–2000*. U.S. Naval Research Laboratory Rep. NRL/MR/7540-02-16, 22 pp.
- Du, Y., S.-P. Xie, G. Huang, and K. Hu, 2009: Role of air-sea interaction in the long persistence of El Niño-induced North Indian Ocean warming. *J. Climate*, **22**, 2023–2038.
- Du, Y., L. Yang, and S.-P. Xie, 2011: Tropical Indian Ocean influence on Northwest Pacific tropical cyclones in summer following strong El Niño. *J. Climate*, **24**, 315–322.
- Emanuel, K., and D. S. Nolan, 2004: Tropical cyclone activity and the global climate system. *Preprints, 26th Conference on Hurricanes and Tropical Meteorology*, Miami, FL, Amer. Meteor. Soc., 240–241.
- England, M. H., S. McGregor, P. Spence, G. A. Meehl, A. Timmermann, W. Cai, A. S. Gupta, M. J. McPhaden, A. Purich, and A. Santoso, 2014: Recent intensification of wind-driven circulation in the Pacific and the ongoing warming hiatus. *Nat. Climate Change*, **4**, 222–227.
- Gill, A. E., 1980: Some simple solutions for heat-induced tropical circulation. *Quart. J. Roy. Meteor. Soc.*, **106**, 447–462.
- Hong, C.-C., Y.-K. Wu, T. Li, and C.-C. Chang, 2014: The climate regime shift over the Pacific during 1996/1997. *Climate Dyn.*, **43**, 435–446.
- Hong, C.-C., Y.-K. Wu, and T. Li, 2016: Influence of climate regime shift on the interdecadal change in tropical cyclone activity over the Pacific Basin during the middle to late 1990s. *Climate Dyn.*, **7**, 2587–2600.
- Hu, C., S. Yang, Q. Wu, T. Zhang, C. Zhang, Y. Li, K. Deng, T. Wang, and J. Chen, 2016: Reinspecting two types of El Niño: A new pair of Niño indices for improving real-time ENSO monitoring. *Climate Dyn.*, **47**, 4031–4049.
- Hu, C., C. Zhang, S. Yang, D. Chen, and S. He, 2018: Perspective on the northwestward shift of autumn tropical cyclogenesis locations over the western North Pacific from shifting ENSO. *Climate Dyn.*, **51**, 2455–2465.
- Huang, B., P. W. Thorne, T. M. Smith, W. Liu, J. Lawrimore, V. F. Banzon, H.-M. Zhang, T. C. Peterson, and M. Menne, 2016: Further exploring and quantifying uncertainties for extended reconstructed sea surface temperature (ERSST) Version 4 (v4). *J. Climate*, **29**, 3119–3142.
- Huang, B., V. F. Banzon, E. Freeman, J. Lawrimore, W. Liu, T. C. Peterson, T. M. Smith, P. W. Thorne, S. D. Woodruff, and H.-M. Zhang, 2015: Extended reconstructed sea surface temperature version 4 (ERSST.v4). Part I: Upgrades and intercomparisons. *J. Climate*, **28**, 911–930.
- Jiang, X., M. Zhao, and D. E. Waliser, 2012: Modulation of tropical cyclones over the eastern Pacific by the intraseasonal variability simulated in an AGCM. *J. Climate*, **25**, 6524–6538.
- Kalnay, E., M. Kanamitsu, R. Kistler, W. Collins, D. Deaven, L. Gandin, M. Iredell, S. Saha, G. White, J. Woollen, Y. Zhu, M. Chelliah, W. Ebisuzaki, W. Hig-

- gins, J. Janowiak, K. C. Mo, C. Ropelewski, J. Wang, A. Leetmaa, R. Reynolds, R. Jenne, and D. Joseph, 1996: The NCEP/NCAR 40-year reanalysis project. *Bull. Amer. Meteor. Soc.*, **77**, 437–471.
- Kao, H.-Y., and J.-Y. Yu, 2009: Contrasting eastern-Pacific and central-Pacific types of ENSO. *J. Climate*, **22**, 615–632.
- Karloski, J. M., and C. Evans, 2016: Seasonal influences upon and long-term trends in the length of the Atlantic hurricane season. *J. Climate*, **29**, 273–292.
- Kendall, M. G., 1975: *Rank Correlation Methods*. Charles Griffin, London, 202 pp.
- Kim, D., H.-S. Kim, D.-S. R. Park, and M.-S. Park, 2017: Variation of the tropical cyclone season start in the western North Pacific. *J. Climate*, **30**, 3297–3302.
- Kim, H.-S., G. A. Vecchi, T. R. Knutson, W. G. Anderson, T. L. Delworth, A. Rosati, F. Zeng, and M. Zhao, 2014: Tropical cyclone simulation and response to CO<sub>2</sub> doubling in the GFDL CM2.5 high-resolution coupled climate model. *J. Climate*, **27**, 8034–8054.
- Klotzbach, P. J., 2007: Recent developments in statistical prediction of seasonal Atlantic basin tropical cyclone activity. *Tellus A*, **59**, 511–518.
- Kosaka, Y., and S.-P. Xie, 2013: Recent global-warming hiatus tied to equatorial Pacific surface cooling. *Nature*, **501**, 403–407.
- Lander, M. A., 1994: An exploratory analysis of the relationship between tropical storm formation in the western North Pacific and ENSO. *Mon. Wea. Rev.*, **122**, 636–651.
- Landsea, C. W., 2007: Counting Atlantic tropical cyclones back to 1900. *Eos*, **88**, 197–208.
- Landsea, C. W., G. A. Vecchi, L. Bengtsson, and T. R. Knutson, 2010: Impact of duration thresholds on Atlantic tropical cyclone counts. *J. Climate*, **23**, 2508–2519.
- L'Heureux, M. L., K. Takahashi, A. B. Watkins, A. G. Barnston, E. J. Becker, T. E. Di Liberto, F. Gamble, J. Gottschalck, M. S. Halpert, B. Huang, K. Mosquera-Vasquez, and A. T. Wittenberg, 2017: Observing and predicting the 2015/16 El Niño. *Bull. Amer. Meteor. Soc.*, **98**, 1363–1382.
- Liu, K. S., and J. C. L. Chan, 2013: Inactive period of western North Pacific tropical cyclone activity in 1998–2011. *J. Climate*, **26**, 2614–2630.
- Liu, Y., and G. Chen, 2018: Intensified influences of the ENSO Modoki on boreal summer tropical cyclone genesis over the western North Pacific since the early 1990s. *Int. J. Climatol.*, **38**, e1258–e1265.
- Mann, H. B., 1945: Non-parametric test against trend. *Econometrica*, **13**, 245–259.
- Mann, H. B., and D. R. Whitney, 1947: On a test of whether one of two random variables is stochastically larger than the other. *Ann. Math Stat.*, **18**, 50–60.
- Matsuno, T., 1966: Quasi-geostrophic motions in the equatorial area. *J. Meteor. Soc. Japan*, **44**, 25–43.
- Maue, R. N., 2011: Recent historically low global tropical cyclone activity. *Geophys. Res. Lett.*, **38**, L14803, doi: 10.1029/2011GL047711.
- Newell, R. E., J. W. Kidson, D. G. Vincent, and G. J. Boer, 1972: *The General Circulation of the Tropical Atmosphere and Interactions with Extratropical Latitudes: Vol. 1*. MIT Press, 320 pp.
- Song, J.-J., Y. Wang, and L. Wu, 2010: Trend discrepancies among three best track data sets of western North Pacific tropical cyclones. *J. Geophys. Res.*, **115**, D12128, doi:10.1029/2009JD013058.
- Takaya, Y., Y. Kubo, S. Maeda, and S. Hirahara, 2017: Prediction and attribution of quiescent tropical cyclone activity in the early summer of 2016: Case study of lingering effects by preceding strong El Niño events. *Atmos. Sci. Lett.*, **18**, 330–335.
- Tao, L., L. Wu, Y. Wang, and J. Yang, 2012: Influences of tropical Indian Ocean warming and ENSO on tropical cyclone activity over the western North Pacific. *J. Meteor. Soc. Japan*, **90**, 127–144.
- Tu, J.-Y., C. Chou, and P.-S. Chu, 2009: The abrupt shift of typhoon activity in the vicinity of Taiwan and its association with western North Pacific–East Asian climate change. *J. Climate*, **22**, 3617–3628.
- Verdon, D. C., and S. W. Franks, 2006: Long-term behaviour of ENSO: Interactions with the PDO over the past 400 years inferred from paleoclimate records. *Geophys. Res. Lett.*, **33**, L06712, doi:10.1029/2005GL025052.
- Wang, B., and J. C. L. Chan, 2002: How strong ENSO events affect tropical storm activity over the western North Pacific. *J. Climate*, **15**, 1643–1658.
- Wang, B., R. Wu, and X. Fu, 2000: Pacific–East Asia teleconnection: How does ENSO affect East Asian climate? *J. Climate*, **13**, 1517–1536.
- Wang, C., and L. Wu, 2016: Interannual shift of the tropical upper-tropospheric trough and its influence on tropical cyclone formation over the western North Pacific. *J. Climate*, **29**, 4203–4211.
- Wilcoxon, F., 1945: Individual comparisons by ranking methods. *Biom. Bull.*, **1**, 80–83.
- Wu, L., and H. Zhao, 2012: Dynamically derived tropical cyclone intensity changes over the western North Pacific. *J. Climate*, **25**, 89–98.
- Wu, L., C. Wang, and B. Wang, 2015: Westward shift of western North Pacific tropical cyclogenesis. *Geophys. Res. Lett.*, **42**, 1537–1542.
- Xiang, B., B. Wang, and T. Li, 2013: A new paradigm for the predominance of standing central Pacific warming after the late 1990s. *Climate Dyn.*, **41**, 327–340.
- Xie, S.-P., K. Hu, J. Hafner, H. Tokinaga, Y. Du, G. Huang, and T. Sampe, 2009: Indian Ocean capacitor effect on Indo-western Pacific climate during the summer following El Niño. *J. Climate*, **22**, 730–747.
- Xie, S.-P., Y. Kosaka, Y. Du, K. Hu, J. S. Chowdary, and G. Huang, 2016: Indo-western Pacific ocean capacitor and coherent climate anomalies in post-ENSO summer: A review. *Adv. Atmos. Sci.*, **33**, 411–432.

- Zhan, R., Y. Wang, and X. Lie, 2011: Contributions of ENSO and east Indian Ocean SSTA to the interannual variability of northwest Pacific tropical cyclone frequency. *J. Climate*, **24**, 509–521.
- Zhao, H., and C. Wang, 2016: Interdecadal modulation on the relationship between ENSO and typhoon activity during the Late Season in the western North Pacific. *Climate Dyn.*, **47**, 315–328.
- Zhao, H., and C. Wang, 2018: On the relationship between ENSO and tropical cyclones in the western North Pacific during the boreal summer. *Climate Dyn.*, **52**, 275–288.
- Zhao, H., L. Wu, and W. Zhou, 2010: Assessing the influence of the ENSO on tropical cyclone prevailing tracks in the western North Pacific. *Adv. Atmos. Sci.*, **27**, 1361–1371.
- Zhao, H., L. Wu, and W. Zhou, 2011: Interannual changes of tropical cyclone intensity in the western North Pacific. *J. Meteor. Soc. Japan*, **89**, 243–253.
- Zhao, H., P.-S. Chu, P.-C. Hsu, and H. Murakami, 2014: Exploratory analysis of extremely low tropical cyclone activity during the late season of 2010 and 1998 over the western North Pacific and the South China Sea. *J. Adv. Model Earth Syst.*, **6**, 1141–1153.
- Zhao, H., R. Yoshida, and G. B. Raga, 2015a: Impact of the Madden-Julian oscillation on western North Pacific tropical cyclogenesis associated with large-scale patterns. *J. Appl. Meteor. Climatol.*, **54**, 1413–1429.
- Zhao, H., X. Jiang, and L. Wu, 2015b: Modulation of northwest Pacific tropical cyclone genesis by the intraseasonal variability. *J. Meteor. Soc. Japan*, **93**, 81–97.
- Zhao, H., X. Duan, G. B. Raga, and F. Sun, 2017: Potential large-scale forcing mechanisms driving enhanced North Atlantic tropical cyclone activity since the mid-1990s. *J. Climate*, **31**, 1377–1397.
- Zhang, Q., L. Wu, and Q. Liu, 2009: Tropical cyclone damages in China 1983–2006. *Bull. Amer. Meteor. Soc.*, **90**, 489–495.